Beyond-pair interactions in the Pd-H$_2$ system

Beyond-pair interactions in the Pd–H$_2$ system

C E Buckley†, J F Dobson† and M A Poyser‡

† Faculty of Science and Technology, Griffith University, Brisbane 4111, Australia
‡ Department of Physics, Joule Laboratory, University of Salford, Greater Manchester M5 4WT, UK

Abstract. By using a mean-field approximation we give a semianalytical method for reducing data on metal–hydrogen systems, which allows for hydrogen–hydrogen (H–H) interactions beyond the level of pair interactions. Interactions up to the triplet level are explicitly included here, although the method allows for interactions up to any finite order. The model fits low-concentration data at one temperature and then predicts pressures, lattice expansion and various energies as functions of concentrations for a range of temperatures. A Monte Carlo simulation is used to lend support to the approximate validity of the mean-field approximation for calculating the entropy in the regime of low concentrations. We find an increasingly negative average triplet interaction energy as the H concentration is increased. Although the mean-field approach is not an adequate description of clustering phenomena leading to the α–β phase transition, nevertheless our finding of a more negative triplet energy with increased concentration may indicate the importance of beyond-pair interactions in the phase transition.

1. Introduction

Even though there has been extensive theoretical investigation into the absorption of hydrogen in palladium, many gaps in our knowledge of the system still remain. The models used to describe the Pd–H$_2$ system include the quasi-chemical model [1, 2], Monte Carlo techniques [3], elastic continuum theory [4], effective-medium theory [5], local-density approximations [6] and molecular dynamics [7]. Given some assumed microscopic interaction between the hydrogen atoms, the simplest model for the statistical mechanics of these systems is the mean-field lattice gas model [8]. This is usually combined with the assumption of pair interactions between hydrogen atoms, often restricted to allow nearest-neighbour (NN) interactions only. It is known from lattice statics theory that hydrogen atoms in a metallic lattice experience long-range strain-mediated interactions which go beyond a sum of pairwise interactions. In this paper we extend the mean-field treatment by allowing pair, triplet and in principle higher interactions between the hydrogen atoms. The intention here is not to formulate a 'supermodel', which describes all the properties of the Pd–H$_2$ system accurately, but instead to see how beyond-pair interactions between hydrogen atoms can be treated in a semi-analytical fashion.

Our philosophy is to assume that the microscopic energy of a metal–hydrogen system is the sum of the site occupation energies together with the pair, triplet, quadruplet, ... n-tuplet terms. We then use a mean-field model to show that, at a low hydrogen concentration r, the effects of these terms on thermodynamic quantities go as $1, r, r^2, r^3$, etc. Hence this hierarchy of interactions can be truncated in the low-concentration α-phase where r is small. This model, which we will term the minimization model, was carried out in practice up to triplet hydrogen interactions, as well as incorporating the experimentally measured change

in the lattice parameter a [9]. In this model the Helmholtz free energy is minimized with respect to both r and ϕ (where ϕ is the dimensionless change $\Delta V / V_0$ in lattice volume), with the desired effect of calculating both the thermally averaged site potential and the thermally averaged interaction energies in terms of r in the α-phase (i.e. when r is small). Some clues concerning the nature of the H–H interaction at the onset of the $\alpha \to \beta$ transition are also obtained using the minimization model.

2. Minimization model

We seek a model which will account for lattice expansion and be able to calculate concentration-dependent thermal averages. The minimization model is constructed to account for the interaction between a H atom and another H atom anywhere in the lattice (pairwise interaction), and the interaction between a H atom and two other H atoms anywhere in the lattice (triplet interaction). Higher interactions are allowed but are not included in the numerical work. The model also incorporates an experimentally determined concentration-dependent change in the lattice parameter [9]. Direct thermal expansion is not explicitly considered as it is usually negligible compared with the hydrogen-induced lattice strain.

The results of mean-field theory (see appendix 1 for a variational derivation) can be qualitatively understood by treating each hydrogen site as independent: the probability that it is occupied is then

$$\theta = r = \frac{\exp[-\beta(\bar{\varepsilon} - \bar{\mu})]}{1 + \exp[-\beta(\bar{\varepsilon} - \bar{\mu})]}. \tag{1}$$

Here the effective (thermally averaged) site potential $\bar{\varepsilon}$ consists of the microscopic energy ε of an isolated hydrogen atom in the lattice, plus a thermally averaged contribution from interaction with other hydrogen atoms:

$$\bar{\varepsilon} = \varepsilon + \bar{V}_2 r + \frac{1}{2!}\bar{V}_3 r^2 + \cdots. \tag{2}$$

$\bar{\varepsilon}$ depends on the average occupation r of other sites, via a sum of pair energies, triplet energies, etc, over all separations R:

$$\bar{V}_2 = \sum_R E^{(2)}(0, R) \tag{3}$$

$$\bar{V}_3 = \sum_{R,R'} E^{(3)}(0, R, R'). \tag{4}$$

In (3) and (4) the bare (non-thermally averaged) pair, triplet, ..., energies $E^{(2)}$, $E^{(3)}$, ... are defined in appendix 2; they can be derived in principle from microscopic theories applied to the low-concentration regime. The effective chemical potential in (1) is

$$\bar{\mu} = \tfrac{1}{2}\mu(H_2, \text{gas}) + 3k_B T \ln Z_{\text{vib}} \tag{5}$$

where $\mu(H_2, \text{gas})$ is the chemical potential of H_2 gas outside the metal and

$$Z_{\text{vib}} = [2\sinh(\beta\hbar\omega/2)]^{-1} \tag{6}$$

is the partition function for a 1D harmonic oscillator; we have assumed an Einstein model for the lattice vibrations, with frequency ω.

A more detailed discussion of equations (1)–(6) is given in appendix 1, where we also treat the case of more than one type of hydrogen site (e.g. octahedral and tetrahedral in the case of Pd–H). In equations (1)–(6) we have used the experimental fact [7] that only one type of site (octahedral, labelled $j = 1$ in appendix 1) is significantly occupied in the Pd–H_2 system below $T = 600$ K. This allows us to suppress the index j of the appendix and thus to use a single fractional concentration $r \equiv \theta$, which is also the probability of site occupation. In appendix 1 it is also shown that the internal energy (thermally averaged total energy) per hydrogen atom in the same mean-field approximation is

$$U = \varepsilon r + \frac{1}{2!}\bar{V}_2 r^2 + \frac{1}{3!}\bar{V}_3 r^3 + O(r^4) \tag{7}$$

while the entropy per H atom is the 'ideal' value given by

$$S = -k_B[(1 - r)\ln(1 - r) + r \ln r]. \tag{8}$$

In order to account for the observed [9] lattice expansion under hydrogen absorption we express the site energy ε, the pairwise interaction energy $\bar{V}_2$ and the triplet interaction energy $\bar{V}_3$ in terms of $\phi(r)$, where the dimensionless lattice expansion parameter ϕ is $\delta(a^3)/a_0^3$, with a the unit-cell side. We calculate energies in the α-phase where r is small; hence a Taylor expansion can be used to express the energies in terms of ϕ:

$$\varepsilon = \varepsilon_{1a} + \varepsilon_{1b}\phi + \varepsilon_{1c}\phi^2 \tag{9}$$

$$\bar{V}_2 = \bar{V}_{2a} + \bar{V}_{2b}\phi + \bar{V}_{2c}\phi^2 \tag{10}$$

$$\bar{V}_3 = \bar{V}_{3a} + \bar{V}_{3b}\phi + \bar{V}_{3c}\phi^2. \tag{11}$$

We stress that the nine parameters ε_{1a}, ε_{1b}, ε_{1c}, $\bar{V}_{2a}$, $\bar{V}_{2b}$, $\bar{V}_{2c}$, $\bar{V}_{3a}$, $\bar{V}_{3b}$ and $\bar{V}_{3c}$ are independent of r and of the temperature T, under the assumptions given in the appendices. All nine parameters could in principle be determined theoretically from a microscopic (non-thermally averaged) analysis of the energy of various configurations of hydrogen in the lattice, as discussed in appendix 2. Here we take a different approach. We shall fit the nine parameters to experimental data at one temperature and then use them to predict system properties at other temperatures. This fitting and prediction are achieved by the standard statistical mechanical procedure of determining the equilibrium state as that which minimizes a mean-field approximation to the Helmholtz free energy.

The total Helmholtz free energy A_{tot} is divided into two components: the free energy A_s of the solid including any absorbed hydrogen and the free energy A_g of the hydrogen gas. To describe thermal equilibrium we minimize A_{tot} with respect to independent variations in ϕ and r:

$$A_{tot} = A_s + A_g \tag{12}$$

$$\frac{\partial A_{tot}}{\partial r} = 0 \tag{13}$$

$$\frac{\partial A_{tot}}{\partial \phi} = 0 \tag{14}$$

$$A_s = U_s - T S_s + A_{vib}. \tag{15}$$

U_s and S_s are given by equations (7) and (8) and the vibrational contribution A_{vib} to the free energy is

$$A_{vib} = -3k_B \, \text{Tr}(\ln Z_{vib}) \tag{16}$$

where Z_{vib} is given by (6).

We differentiate (7), (8) and (16) with respect to r to find $\partial A_s / \partial r$ and then add this to $\partial A_g / \partial r$ to give the partial derivative with respect to r of the total free energy per lattice site, which must be zero by (13):

$$0 = \frac{\partial A_{tot}}{\partial r} = \bar{\varepsilon} + k_B T \ln \left(\frac{r}{1-r} \right) - 3k_B T \ln Z_{vib} - \tfrac{1}{2}\mu_{H_2}. \tag{17}$$

Setting the right-hand side of equation (17) to zero is equivalent to equation (1) and amounts physically to demanding that the hydrogen chemical potential is the same for the gas and the solid. In order to account for the hydrogen-induced lattice expansion we substitute the expression for $\bar{\varepsilon}$ from equations (9)–(11) into (2) and then substitute equation (2) into (17). This gives

$$\frac{\partial A_{tot}}{\partial r} = 0 = \varepsilon_{1a} + \varepsilon_{1b}\phi + \varepsilon_{1c}\phi^2 + \bar{V}_{2a}r + \bar{V}_{2b}r\phi + \bar{V}_{2c}r\phi^2 + \tfrac{1}{2}\bar{V}_{3a}r^2 + \tfrac{1}{2}\bar{V}_{3b}r^2\phi + \tfrac{1}{2}\bar{V}_{3c}r^2\phi^2$$

$$- k_B T \ln \left(\frac{1-r}{r} \right) - 3k_B T \ln Z_{vib} - \tfrac{1}{2}\mu_{H_2}. \tag{18}$$

The second condition for equilibrium is that A_{tot} be a minimum with respect to ϕ; this will formally determine the degree of lattice expansion at any temperature, in terms of the nine parameters ε_{1a}, ε_{1b}, ε_{1c}, $\bar{V}_{2a}$, $\bar{V}_{2b}$, $\bar{V}_{2c}$, $\bar{V}_{3a}$, $\bar{V}_{3b}$ and $\bar{V}_{3c}$:

$$0 = \frac{\partial A_{tot}}{\partial \phi} = \frac{\partial A_s}{\partial \phi} + \frac{\partial A_g}{\partial \phi}. \tag{19}$$

It can easily be shown that

$$\frac{\partial A_g}{\partial \phi} = p V_0 \tag{20}$$

where p is the gas pressure and V_0 is the unperturbed volume of the lattice. The partial derivative of the free energy of the solid with respect to ϕ is all that remains to be found. We substitute (9), (10) and (11) into (7), and then substitute (7) and (8) into (15). A partial differentiation of (15) with respect to ϕ, using the assumption that S_s and A_{vib} do not depend explicitly on ϕ, leads to the expression

$$\frac{\partial A_s}{\partial \phi} = \varepsilon_{1b}r + 2\varepsilon_{1c}\phi r + \tfrac{1}{2}\bar{V}_{2b}r^2 + \bar{V}_{2c}\phi r^2 + \tfrac{1}{6}\bar{V}_{3b}r^3 + \tfrac{1}{3}\bar{V}_{3c}\phi r^3. \tag{21}$$

From (19), the condition for equilibrium with respect to changes in lattice constant then becomes

$$\frac{\partial A_{tot}}{\partial \phi} = 0 = \varepsilon_{1b}r + 2\varepsilon_{1c}\phi r + \tfrac{1}{2}\bar{V}_{2b}r^2 + \bar{V}_{2c}\phi r^2 + \tfrac{1}{6}\bar{V}_{3b}r^3 + \tfrac{1}{3}\bar{V}_{3c}\phi r^3 + p V_0. \tag{22}$$

Table 1. The nine parameters which are calculated from the minimization model at $T = 473$ K are used to parametrize the Pd–H$_2$ system in the α-phase in the temperature range 433–553 K. The nine parameters are also used to calculate the energies of the Pd–H$_2$ system in the α-phase.

Parameter symbol	Parameter value (kJ mol^{-1})
ε_{1a}	$-0.664\,729\,0 \times 10$
ε_{1b}	$0.151\,106\,4 \times 10^{-2}$
ε_{1c}	$-0.499\,009\,9 \times 10^3$
$\bar{V}_{2a}$	$-0.400\,827\,4 \times 10^2$
$\bar{V}_{2b}$	$0.359\,584\,0 \times 10^3$
$\bar{V}_{2c}$	$0.239\,583\,4 \times 10^4$
$\bar{V}_{3a}$	$-0.590\,750\,3 \times 10^2$
$\bar{V}_{3b}$	$-0.285\,531\,0 \times 10^{-1}$
$\bar{V}_{3c}$	$-0.645\,559\,8 \times 10^5$

If the nine parameters were known, then equations (18) and (22) could be solved to find the filling factor r, and the dimensionless change in lattice volume ϕ at any desired temperature and gas pressure in the α-phase. Since the nine parameters are not known, equations (18) and (22) are used to establish values for these nine parameters by fitting suitable experimental data from the α-phase. There are nine independent parameters, and these should in principle be determined from $M = 9$ experimental data points. This fit is likely to be too noisy; so a least-squares procedure employing $M > 9$ experimental data points is used.

Equations (18) and (22) can be solved using the following least-squares method. Square equation (18) and add it to the square of equation (22); then sum over M data points. The quantity so constructed is termed χ and it is a measure of the departure between predicted and experimental data:

$$
\sum_{i=1}^{M} \left\{ \left[\varepsilon_{1a} + \varepsilon_{1b}\phi_i + \varepsilon_{1c}\phi_i^2 + \bar{V}_{2a}r_i + \bar{V}_{2b}r_i\phi_i + \bar{V}_{2c}r_i\phi_i^2 + \tfrac{1}{2}\bar{V}_{3a}r_i^2 + \tfrac{1}{2}\bar{V}_{3b}r_i^2\phi_i + \tfrac{1}{2}\bar{V}_{3c}r_i^2\phi_i^2 \right. \right.
$$

$$
\left. - k_B T \ln\left(\frac{1-r_i}{r_i}\right) - 3k_B T \ln(Z_{\text{vib}})_i - \tfrac{1}{2}(\mu_{H_2})_i \right]^2
$$

$$
\left. + \left(\varepsilon_{1b}r_i + 2\varepsilon_{1c}\phi_i r_i + \tfrac{1}{2}\bar{V}_{2b}r_i^2 + \bar{V}_{2c}\phi_i r_i^2 + \tfrac{1}{6}\bar{V}_{3b}r_i^3 + \tfrac{1}{3}\bar{V}_{3c}\phi_i r_i^3 - pV_0 \right)^2 \right\} = \chi.
$$

(23)

We minimized equation (23) with respect to the nine parameters ε_{1a}, ε_{1b}, ε_{1c}, $\bar{V}_{2a}$, $\bar{V}_{2b}$, $\bar{V}_{2c}$, $\bar{V}_{3a}$, $\bar{V}_{3b}$ and $\bar{V}_{3c}$ by demanding that

$$
\frac{\partial\chi}{\partial\varepsilon_{1a}} = 0 \qquad \frac{\partial\chi}{\partial\varepsilon_{1b}} = 0 \qquad \frac{\partial\chi}{\partial\varepsilon_{1c}} = 0 \qquad \frac{\partial\chi}{\partial\bar{V}_{2a}} = 0 \qquad \frac{\partial\chi}{\partial\bar{V}_{2b}} = 0
$$

$$
\frac{\partial\chi}{\partial\bar{V}_{2c}} = 0 \qquad \frac{\partial\chi}{\partial\bar{V}_{3a}} = 0 \qquad \frac{\partial\chi}{\partial\bar{V}_{3b}} = 0 \qquad \frac{\partial\chi}{\partial\bar{V}_{3c}} = 0.
$$

(24)

These nine equations with nine unknowns (the nine parameters) are set up by substituting $M = 20$ (r, ϕ, p) data values [9, 10] into the nine differentiated forms of equation (24). This resulted in a 9×9 set of linear equations which were solved using LU decomposition. The nine parameters obtained in this procedure are shown in table 1; data at $T = 473$ K were used in obtaining the fit.

3. Analysis of the Pd–H$_2$ system in the α-phase, using the nine parameters

The nine parameters just obtained can be used in principle to predict the P–C phase diagrams for the Pd–H$_2$ system at any temperature. Before this can be accomplished, the P–C phase diagram at $T = 473$ K must be calculated and compared with the experimental P–C diagram at this temperature, so that the validity of the nine parameters can be tested. If the fit is good, it implies that the least-squares procedure has been successful.

The following procedure was used to predict $p(r, T)$, given the known values of the nine parameters. Both equation (18) and equation (22) contain p. In equation (18) the pressure is found in the chemical potential μ_H and p is explicit in equation (22). Solving for p in equation (18) gives

$$p = \exp\left(\frac{2}{k_B T}(A\phi^2 + B\phi + C - D)\right) \tag{25}$$

where

$$A = \varepsilon_{1c} + \bar{V}_{2c}r + \tfrac{1}{2}\bar{V}_{3c}r^2 \tag{26}$$

$$B = \varepsilon_{1b} + \bar{V}_{2b}r + \tfrac{1}{2}\bar{V}_{3b}r^2 \tag{27}$$

$$C = \varepsilon_{1a} + \bar{V}_{2a}r + \tfrac{1}{2}\bar{V}_{3a}r^2 - k_B T \ln\left(\frac{1-r}{r}\right) - 3k_B T \ln Z_{\text{vib}} \tag{28}$$

$$D = -\tfrac{1}{2}k_B T\left\{\ln T^{7/2} + \ln\left[\left(\frac{2\pi m k_B}{h^2}\right)^{3/2}\frac{A_m k_B^2}{\hbar^2}\right] - \frac{\varepsilon_D}{k_B T} - \frac{\hbar\omega_{H-H}}{2k_B T}\right.$$

$$\left. - \ln\left[1 - \exp\left(\frac{-\hbar\omega_{H-H}}{k_B T}\right)\right]\right\}. \tag{29}$$

Making p the subject of equation (22) results in

$$p = \frac{1}{V_0}\left(\varepsilon_{1b}r + 2\varepsilon_{1c}\phi r + \tfrac{1}{2}\bar{V}_{2b}r^2 + \bar{V}_{2c}\phi r^2 + \tfrac{1}{6}\bar{V}_{3b}r^3 + \tfrac{1}{3}\bar{V}_{3c}\phi r^3\right). \tag{30}$$

When (30) is equated to (25), the only unknown is ϕ, since the nine parameters and T are known. $\phi(r)$ is calculated using the bisection method and then substituted back into equation (25) to find p.

An excellent fit to the experimental data is found for both the calculated P–C phase diagram and the calculated dimensionless change in lattice volume at $T = 473$ K. This implies that the minimization and least-squares algorithm are working well.

The next logical step was to calculate the P–C isotherm and the dimensionless change in lattice volume in the α-phase at a series of temperatures, using the nine parameters calculated at $T = 473$ K. This was done for the temperature range $T = 433$–553 K. The calculated phase diagrams (open squares) for the temperatures $T = 433$ and 553 K are compared with the experimental phase diagrams (asterisks) in figure 1 ($T = 433$ K) and figure 2 ($T = 553$ K), and the calculated and experimental dimensionless change in lattice
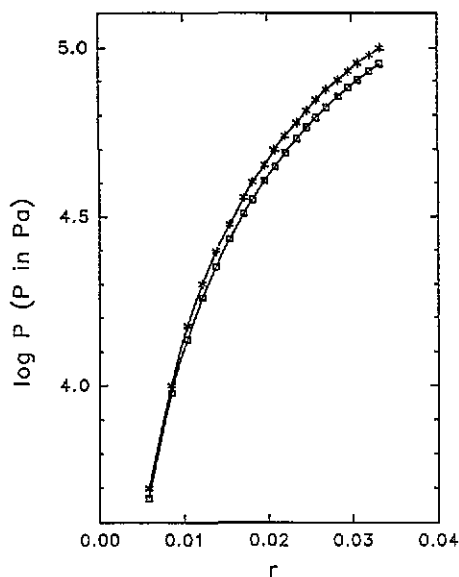
Figure 1. A comparison of the experimental (*) and calculated (□) P–C phase diagrams (see equation (30)) in the α-phase for the Pd–H$_2$ system at $T = 433$ K. The calculated P–C phase diagram at this temperature and other temperatures is determined using the nine parameters derived from the minimization model at $T = 473$ K.
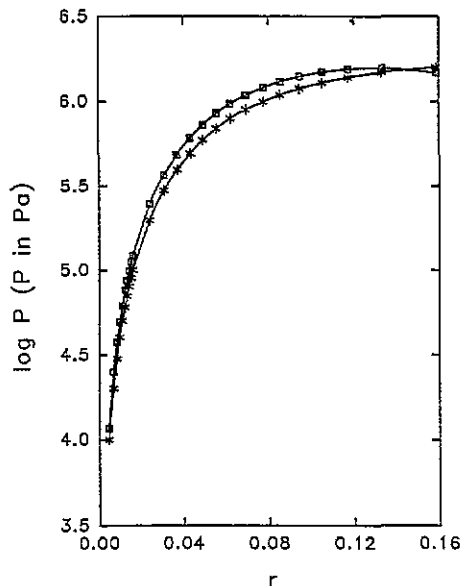
Figure 2. A comparison between the experimental (*) and calculated (□) P–C phase diagrams for the Pd–H$_2$ system in the α-phase at $T = 553$ K.

parameter ϕ at the above temperatures are compared in figure 3 ($T = 433$ K) and figure 4 ($T = 553$ K).

The agreement between experiment and calculation for the P–C phase diagrams is quite good at all temperatures. Temperatures above $T = 473$ K have larger calculated $\log P$ values, except for one value at $T = 553$ K, whereas at $T = 433$ K the calculated values yield slightly lower $\log P$ values. At $T = 553$ K, the last calculated $\log P$ value falls below the experimental value. This is to be expected since the onset of the β-phase at $T = 553$ K is at $r \simeq 0.16$ and the nine parameters were calculated at $T = 473$ K, where r ranged from 0.0045 to 0.0617. Hence the calculated values work well for over twice the range in r at which the nine parameters were calculated.

The agreement between calculated and experimental ϕ is very good at $T = 433$ K (see figure 3) for all concentrations considered and is also very good at $T = 553$ K (see figure 4) up to a concentration of $r \simeq 0.12$, after which the calculated values start to fall away from the experimental results. Even at $r \simeq 0.12$, the error between the calculated and experimental results is only about 8%. Once again there is close agreement between the calculated and experimental results for r-values over twice the magnitude of the r-values at which the nine parameters were calculated.

Since the calculated results of the concentration-dependent pressures and the concentration-dependent dimensionless change in lattice volume are in sufficiently close agreement with the experimental results, an approximate parametrization of the Pd–H$_2$ system in the α-phase in the temperature range $T = 433$–553 K has been achieved. Hence one can have a greater measure of confidence in the validity of the concentration-dependent energies calculated in the next section.
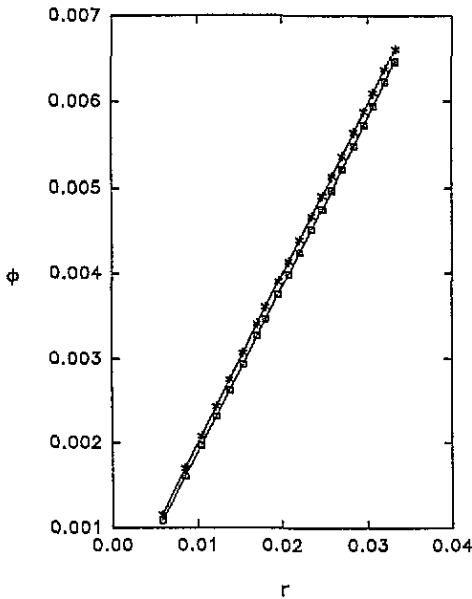
Figure 3. A comparison of the experimental (∗) and calculated (□) dimensionless changes in lattice volume ϕ in the α-phase for the Pd–H$_2$ system at $T = 433$ K. The calculated ϕ (see equations (25) and (30)) at this temperature and other temperatures is determined using the nine parameters derived from the minimization model at $T = 473$ K.
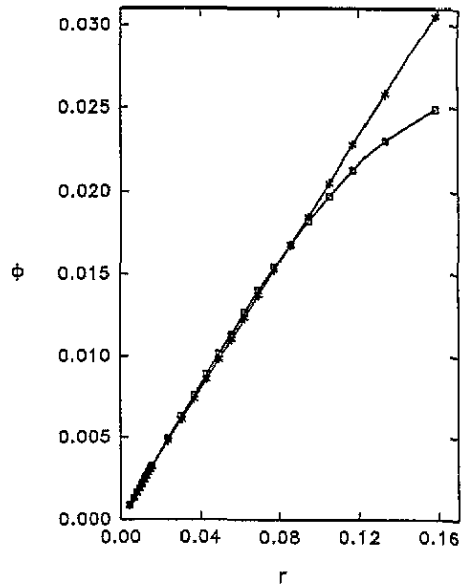
Figure 4. A comparison of the experimental (∗) and calculated (□) dimensionless changes in lattice volume ϕ in the α-phase for the Pd–H$_2$ system at $T = 553$ K.

4. Energy calculations for the Pd–H$_2$ system

The bare site energy ε and the summed pair potentials $\bar{V}_2$ and triplet potentials $\bar{V}_3$ are calculated by substituting the nine parameters into equations (9)–(11). The mean-field potential $\bar{\varepsilon}$ is calculated by substituting these equations into (2). It is useful also to define the effective interaction energy $\bar{V}$. This is the contribution to the mean-field potential $\bar{\varepsilon}$ due to hydrogen–hydrogen interactions. From equation (2), this is

$$\bar{V} = \bar{V}_2 r + \tfrac{1}{2}\bar{V}_3 r^2. \tag{31}$$

$\bar{V}$ is found numerically by substituting equations (10) and (11) into equation (31).

Figures 5, 6 and 7 are plots of ε versus r, $\bar{V}_2$ versus r and $\bar{V}_3$ versus r, respectively, at $T = 473$ K. The pair energy $\bar{V}_2$ is linear in r whereas the site energy ε and the triplet energy $\bar{V}_3$ have a pronounced curvature. All the energies have sensible magnitudes and trends. ε has small negative values and changes very little as r is increased. This is to be expected since the calculation takes place in the α-phase, where the change in the lattice parameter is quite small. The increasing negative trend of ε also has physical significance, since a small expansion of the lattice will compel the octahedral site to increase marginally in size, which in turn will lower the potential of the site.

$\bar{V}_2$ is a negative interaction between H atoms which changes by only 0.05 eV over the range $r = 0.004$–0.06. It must be remembered that $\bar{V}_2$ is not a nearest-neighbour or second-neighbour interaction but is the pairwise interaction with a selected hydrogen atom, summed
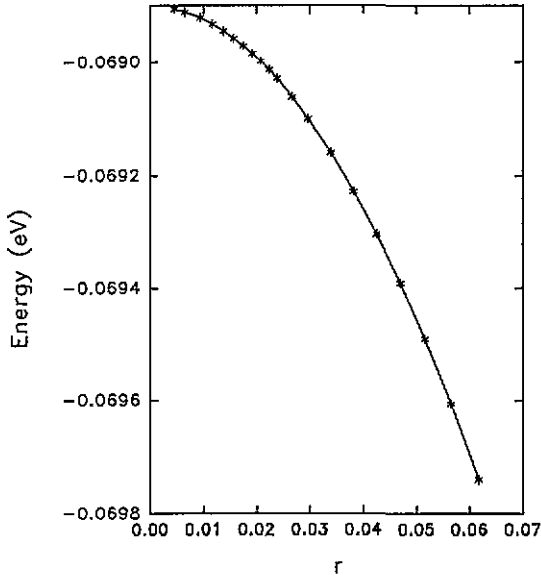
Figure 5. The concentration-dependent site energy ε (see equation (9)) in the α-phase for the Pd–H_2 system at $T = 473$ K. The energies of figures 5–7 are calculated using the minimization model.
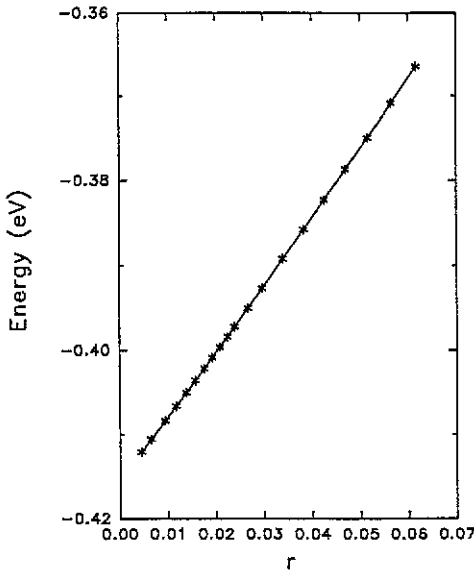

Figure 6. The concentration-dependent effective pairwise interaction energy $\bar{V}_2$ (see equation (10)) in the α-phase for the Pd–H_2 system at $T = 473$ K.
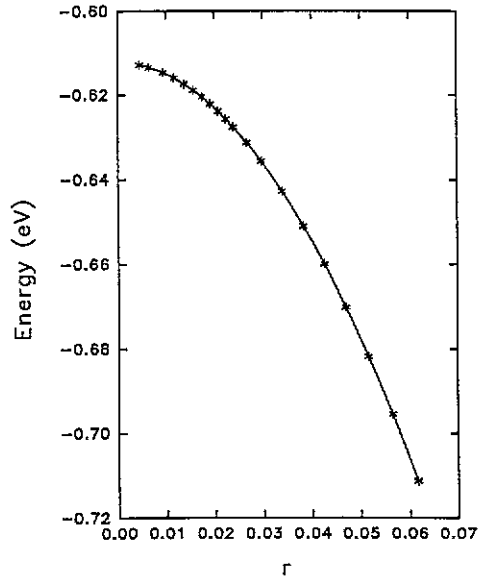
Figure 7. The concentration-dependent effective triplet interaction energy $\bar{V}_3$ (see equation (11)) in the α-phase for the Pd–H_2 system at $T = 473$ K.

over all other H atoms in the lattice. The fact that $\bar{V}_2$ samples all separations equally is due to our lowest-order ('point') mean-field approximation. As a result, the negative value of

$\bar{V}_2$ strictly implies only that this term tends to attract more hydrogen atoms into the lattice out of the gas, if hydrogen atoms are already absorbed. If it is known on microscopic or other grounds that $E^{(2)}(0, R)$ falls off monotonically with $|R|$, then one can also deduce that a negative value of $\bar{V}_2$ implies an attractive pair interaction between hydrogen atoms, which would tend to favour clustering of hydrogen atoms once they are inside the lattice. This conclusion cannot be rigorously deduced from our mean-field analysis alone, however. Nevertheless, with this caveat, we shall describe negative pair and triplet interactions as 'attractive'. The attractive pairwise interaction is consistent with the literature [6, 7, 9, 11]. The major advantage of this model is that it takes into account the lattice expansion, and the pairwise interaction energy is given in terms of the hydrogen occupation.

$\bar{V}_3$ is also a negative ('attractive') interaction, which becomes more negative as r increases. To our knowledge a concentration-dependent triplet interaction for H in Pd or any other metal or intermetallic has not yet been published. Some support for our finding is provided by the work of Oates and Stoneham [12] who calculated some concentration-independent non-pairwise interaction energies for the Pd–H_2 system. They found that these were significant and attractive. Although our model is of a mean-field character and therefore inherently neglects clustering, the increasingly negative trend of the mean triplet energy as the concentration increases suggests that an increasingly attractive beyond-pairs interaction is occurring. One might expect this to play a role in clustering and hence in the transition to the β-phase.

Table 2 compares the values of $\bar{V}_2 r$, $0.5\bar{V}_3 r^2$ and $\bar{V}$ calculated from the minimization model with the H–H interaction energies calculated by other methods [3, 5, 12–14]. We note that values for the pairwise H–H interaction energy calculated from the literature are compared with the quantity $\bar{V}_2 r$ in the minimization model. It is evident from the table that our calculations split the contribution of the total H–H interaction energy into average pairwise interactions and average triplet interactions. The other methods do not calculate the triplet contribution $0.5\bar{V}_3 r^2$ to the total interaction energy $\bar{V}$. The values for the EAM, pair potentials and the harmonic crystal model are evaluated from a H–H interaction energy versus H–H distance graph [13]. The result from the EAM and EMT stem from elastic and direct electronic interactions. Our result for $\bar{V}$ using relatively simple techniques is comparable with the result obtained from the more advanced methods, such as EAM and EMT. No values for a concentration-dependent bare site potential were found in the literature; therefore no comparison with $\varepsilon(r)$ could be made.

Table 2. Comparison of the pairwise interaction and the total H–H interaction energy at a concentration of $r = 0.06$ between that calculated from the minimization model with that calculated from other models [3, 5, 12–14]. The minimization model is the only method which divides the total interaction energy into pairwise and triplet contributions.

Method used	$\bar{V}_2 r$ at $r = 0.06$ (meV)	$0.5\bar{V}_3 r^2$ at $r = 0.06$ (meV)	$\bar{V}$ at $r = 0.06$ (meV)
Embedded atom model (EAM) [13]	−6.36	—	−6.36
Pair potentials [12]	−4.94	—	−4.94
Harmonic crystal model [3]	10.56	—	10.56
Effective-medium theory (EMT) [5]	−15	—	−15
Molecular dynamics [14]	−34.3	—	−34.3
Minimization model	−22	−1.5	−23.5

5. Validity of the mean-field approach

The essence of our lowest-order mean-field theory is the neglect of explicit correlations between hydrogen occupations on different sites. In the variational approach given in appendix 1, this arises by writing joint occupation probabilities explicitly as products of single-site probabilities, within the context of the grand canonical ensemble of statistical mechanics. This 'point approximation' can be improved by splitting the lattice into disjoint clusters and writing the probability of a hydrogen configuration as the product of separate terms for each cluster; this results in a form of the Bethe approximation, which should give a more reasonable description of the clustering phenomena arising near the $\alpha \rightarrow \beta$-phase transition. By using the point approximation rather than a higher cluster approximation, we clearly lose the ability to describe this clustering transition in a direct fashion. Nevertheless the lowest-order mean-field theory is known to give semiquantitative information away from the phase transition, in three dimensions.

In the variational approach, one assumes that the microscopic energy is known as a function of the microscopic hydrogen configuration. The approximations arise in evaluation of thermally averaged quantities: the entropy (which equals the ideal or non-interacting entropy in this approximation) and, separately, the internal energy. Then one forms the free energy from these quantities (or, in the grand ensemble, the grand potential); by minimizing this, one selects the optimum effective one-particle occupation probability. It is of interest to find which quantity causes the main error in mean-field theory: the entropy or the thermally averaged internal energy. To test this we performed a Monte Carlo calculation of the entropy with near-neighbour and second-neighbour occupation excluded, which is equivalent to assuming an infinite repulsive pair potential at these separations. The results are compared with the ideal entropy in figure 8 at low concentrations r corresponding to the α-phase. The close agreement suggests that the entropy is not the main source of error in the point mean-field approximation. In retrospect this is unsurprising; the likelihood of near-neighbour occupation with random uncorrelated site occupation is of order r^2 which is very small in the α-phase, and hence formal exclusion of these configurations in the Monte Carlo simulation makes little difference over and above the mean-field estimate. On the other hand, one can easily see that the internal energy can be poorly estimated in the mean-field approach. For example, with infinite near-neighbour repulsive energy, the mean-field approach, which fails to exclude near-neighbour occupation, results in an estimate of $+\infty$ for the internal energy U. Thus, in the α-phase it is principally the internal energy, and not the entropy, which causes the main error in mean-field theory. Despite this weakness of the mean-field approximation, it is known that low-order mean-field theory gives increasingly good results as the range of the interaction potential increases. It seems likely that our type of approach could be made to describe the system closer to the α–β transition if a cluster larger than one were used in the variational approach. A small cluster could give an improved accounting of the strong short-range hydrogen–hydrogen interactions, and the long-range strain-induced pair, triplet and higher interactions can be expected to be well described by mean-field theory. Such an approach may be worth pursuing in the future, but the present work deals only with a cluster of one.

6. Summary and discussion

This paper has been concerned with parametrizing the Pd–H_2 system in a specific temperature range as well as calculating concentration-dependent doublet and triplet
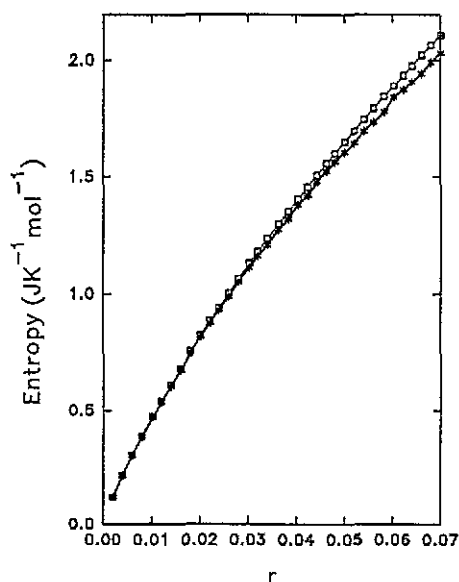
Figure 8. A comparison of the ideal entropy (□) and the entropy calculated using Monte Carlo (∗) methods. The entropy calculated using Monte Carlo assumes infinite repulsion between H atoms within a radius out to second-nearest-neighbour distances. Even at the concentration at which the $\alpha \to \beta$-phase transition occurs in the Pd–H₂ system ($r = 0.0617$) at $T = 473$ K, the difference between the two entropies is only 2.7%.

energies. We have shown that H–H pair interactions, triplet H–H–H interactions and in principle higher hydrogen–hydrogen interactions can be treated in a semianalytical fitting procedure provided that one uses the mean-field approximation and works in the regime of low hydrogen concentrations; the essence of this fit is that the mean-field approximation leads to an expression, equation (2), for the effective site potential in powers of the hydrogen concentration r. The coefficient of higher powers involve multi-hydrogen interactions. The entropy S and internal energy U also have expansions in powers of r (see equations (7) and (8)) whose coefficients are unequivocally related via our mean-field theory, to those of the effective site potential $\bar{\varepsilon}$ (equation (2) or equation (A1.20) in general). A similar expansion in powers of the occupation probability r also follows for the Helmholtz free energy $A = U - TS$.

We have found and tabulated the coefficients in mean-field-derived fit expressions for the pressure, effective potentials, energies and lattice expansion of Pd–H (table 1) and have shown they provide a comprehensive fit to experimental data for Pd–H in the α-phase in the temperature range 433–533 K. Lower-quality fits were found only for high T- and r-values more than twice the values for which the fitting was done. To investigate the appropriateness of the mean-field approach we have also performed a Monte Carlo calculation for the entropy. Interestingly, we find only fairly small differences from the mean-field (ideal) results for the entropy in the low-concentration α-phase. By contrast, for the high-concentration β-phase, the mean-field expressions for S (equation (8)) and U (equation (7)) could not be used; for these higher concentrations the ideal entropy and the internal energy would differ markedly from the true entropy and internal energy of the system.

Although the number of fitting parameters in our best fits is large (equal to 9), the

advantage of the theoretically derived fit expressions, over arbitrary fitting functions, is that the potentials and energies in the fit expressions have simple physical interpretations. In particular the average (mean-field) potential energy of H on a lattice site can be divided into contributions from a concentration-dependent site energy $\bar{\varepsilon}$, an effective average pair potential $\bar{V}_2$, an effective triplet potential $\bar{V}_3$ and so on. By making a clear distinction between these potentials we have found indirect evidence that beyond-pairwise interactions may be important in bringing about the $\alpha \to \beta$-phase transition.

While our mean-field fits are quite good, it appears that the large size of the cross coefficients $\bar{V}_{2b}$, $\bar{V}_{2c}$, $\bar{V}_{3b}$ and $\bar{V}_{3c}$ between the pair and triplet interactions and the lattice expansion may indicate that our formalism is being forced to fit phenomena to which it is not ideally suited. One possibility is that one should restrict the lattice expansion coefficients (appearing in (9)–(11) as pre-factors of powers of ϕ) to occur only in the lowest-order term in the r expansion, and instead of higher lattice expansion coefficients one could introduce correlations (i.e. clustering) into the formalism by use of a Bethe or related *Ansatz*. It seems possible that a more natural fit to the data, possibly with fewer coefficients, would thus be obtained [15].

In principle the minimization model can be applied to other systems such as the LaNi$_5$–H$_2$ system. This particular metal hydride system exhibits a large difference in the hysteresis between that of an initial cycle and a well activated cycle [16]. Knowledge of the magnitude of the site energy and interaction energies at the concentration where the $\alpha \to \beta$-phase transition occurs for these two cycles may provide insight into which energy is chiefly responsible for the large difference between the hysteresis of the two cycles. A forthcoming publication will describe the results obtained when the minimization model is applied to the LaNi$_5$–H$_2$ system in an attempt to interpret the influence of microstructure on hysteresis.

Acknowledgments

Appendix 1. Model for energetics and statistical mechanics of hydrogen in metal

Let the metal have N_j available H sites of type j. (In Pd–H, $j = 1$ represents octahedral sites while $j = 2$ represents tetrahedral sites.) An occupational state of hydrogen on the lattice is described by a set of occupation numbers $n_{j,\alpha} = 0$ or 1 where $1 \leqslant \alpha \leqslant N_j$, and α labels the different sites of a given type. A set of numbers $\{n_{j,\alpha}\}$ completely describes which available lattice sites are occupied by hydrogen. The lattice will have a unique distorted shape corresponding to each set $\{n_{j,\alpha}\}$. The energy of the whole lattice, including distortions but excluding lattice vibration which we treat later via a simple model, is

$$E(\{n_{j\alpha}\}) = \sum_{j\alpha} n_{j\alpha} E^{(1)}(j\alpha) + \frac{1}{2!} \sum_{j\alpha, j'\alpha'} n_{j\alpha} n_{j'\alpha'} E^{(2)}(j\alpha, j'\alpha')$$

$$+ \frac{1}{3!} \sum_{j\alpha, j'\alpha', j''\alpha''} n_{j\alpha} n_{j'\alpha'} n_{j''\alpha''} E^{(3)}(j\alpha, j'\alpha', j''\alpha'') + \cdots . \tag{A1.1}$$

It is shown in appendix 2 that the site, pair, triplet, quadruplet, ..., energies, $E^{(1)}$, $E^{(2)}$, $E^{(3)}$, etc, can be defined so as to be unique, at least in the low-concentration regime. Without a microscopic model there is no particular reason to assume $E^{(3)} < E^{(2)}$, etc. We shall show, however, that the *effect* of the higher-order interactions is small at low concentrations, provided that one uses mean-field theory. From microscopic considerations it seems likely that strong effective interactions between hydrogen atoms, mediated directly by electron cloud distortion are of a fairly short range nature [17]. The long-range part is expected to be mediated by elastic forces of the lattice-statics variety [18]. (These of course also have an ultimate electronic origin but less directly so than the above-mentioned short-range H–H forces, in that electronically initiated short-range forces between hydrogen atoms and the metal ions are sufficient to obtain long-range effective lattice-statics forces between the hydrogen atoms.) For some of our work it is also useful to define the $\{E^{(n)}\}$ to have been determined by minimizing the electronic energy with respect to lattice distortions at a particular fixed volume, or equivalently at a fixed value a of the average lattice cell dimension. Thus the $\{E^{(n)}\}$ are dependent on a; so we have, for example, $E^{(3)}(j, \alpha, j', \alpha', j'', \alpha'' : a)$. This allows us to discuss the expansion of the lattice. (At high H concentrations it might be better to define the energies at a fixed average conduction electron density, but we do not do this here.)

We assume that the system of metal plus absorbed gas is in contact with a heat and particle reservoir at temperature $T = (k_B \beta)^{-1}$ and H (or D) atom chemical potential μ. In practice the reservoir is the H_2 or D_2 gas in contact with the metal, and by minimizing the total Helmholtz free energy with respect to transfer of gas molecules into the atomic form inside the metal, using $2N(H_2, \text{gas}) + N(H, \text{metal}) = \text{constant}$, one obtains

$$\mu = \tfrac{1}{2}\mu(H_2, \text{gas}). \qquad (A1.2)$$

For the lattice vibrations we assume an isotropic Einstein model in which the H atom at site $(j\alpha)$ vibrates independently in three dimensions at frequency $\omega_{j\alpha}$ and hence contributes a vibrational energy $(v_{j\alpha x} + v_{j\alpha y} + v_{j\alpha z} + \tfrac{3}{2})\hbar\omega_{j\alpha}$, where $v_{j\alpha x}$, $v_{j\alpha y}$ and $v_{j\alpha z}$ can independently take values $0, 1, 2, 3, \ldots$. The exact equilibrium probability distribution for the lattice hydrogen state $\{n_{j\alpha}, v_{j\alpha x}, v_{j\alpha y}, v_{j\alpha z}\} \equiv \{n_{j\alpha}, v_{j\alpha}\}$ is the Gibbs or grand canonical distribution

$$p(\{n_{j\alpha}, v_{j\alpha}\}) = Q_0^{-1} \exp\left(\beta\mu N - \beta E(\{n_{j\alpha}\}) - \beta \sum_{j\alpha} n_{j\alpha}\hbar\omega_{j\alpha}(v_{j\alpha x} + v_{j\alpha y} + v_{j\alpha z} + \tfrac{3}{2}) \right)$$

$$(A1.3)$$

where

$$N = \sum_{j,\alpha} n_{j,\alpha} \qquad (A1.4)$$

is the total number of absorbed hydrogen atoms and where the grand partition function Q_0 is the sum, over all states $\{n_{j\alpha}, v_{j\alpha}\}$, of the exponential factor on the right-hand side of (A1.3). Here we are not interested in the individual vibrational levels $v_{j\alpha}$. Summing over all these quantities we obtain the probability of a hydrogen configuration $\{n_{j\alpha}\}$:

$$p(\{n_{j\alpha}\}) = Q^{-1} \exp\left(\beta\mu N - \beta E(\{n_{j\alpha}\}) \prod_{j\alpha} [Z_{\text{vib}}(\beta, \omega_{j\alpha})]^{3n_{j\alpha}} \right) \qquad (A1.5)$$

where

$$Q = \sum_{\{n_{j,\alpha}\}} \exp[\beta\mu N - \beta E(\{n_{j,\alpha}\})] \prod_{j\alpha} [Z_{\mathrm{vib}}(\beta, \omega_{j\alpha})]^{3n_{j\alpha}} \tag{A1.6}$$

is the configurational grand partition function or Gibbs sum for the absorbed hydrogen system. In (A1.5) and (A1.6),

$$Z_{\mathrm{vib}}(\beta, \omega) = \sum_{\nu=0}^{\infty} \exp[-\beta\hbar\omega(\nu + \tfrac{1}{2})] = \frac{1}{2\sinh(\beta\hbar\omega/2)} \tag{A1.7}$$

is the partition function of a one-dimensional quantal harmonic oscillator.

By the method of Lagrange multipliers, it is easily shown that (A1.5) is the distribution which minimizes the quantity

$$\Omega = U - TS - \mu N - k_{\mathrm{B}}T \sum_{j\alpha} 3\ln[Z_{\mathrm{vib}}(\beta, \omega_{j\alpha})]n_{j\alpha} \tag{A1.8}$$

subject to the normalization condition

$$\sum_{j\alpha} p(\{n_{j\alpha}\}) = 1. \tag{A1.9}$$

In (A1.8), S is the Kolmogorov expression for the configurational entropy of the interacting hydrogen in the lattice:

$$S = -k_{\mathrm{B}} \sum_{\{n_{j\alpha}\}} p(\{n_{j\alpha}\}) \ln[p(\{n_{j\alpha}\})]. \tag{A1.10}$$

U is the internal energy given by

$$U = \langle E(\{n_{j\alpha}\}) \rangle = \sum_{\{n_{j\alpha}\}} E(\{n_{j\alpha}\}) p(\{n_{j\alpha}\}). \tag{A1.11}$$

The minimum principle (A1.8) allows the introduction of variational approximation schemes, the simplest of which is the usual mean-field approximation in which a joint probability is approximated as a product of one-particle probabilities:

$$p(\{n_{j\alpha}\}) = \prod_{j\alpha} f_{j\alpha}(n_{j\alpha}). \tag{A1.12}$$

Equation (A1.12) implies that occupation probabilities of different sites are independent, i.e. clustering is neglected at this level. (Improved approximations of the Bethe type could be derived by splitting $p(\{n_{j\alpha}\})$ into a product over disjoint cluster terms each involving more than one site. We do not pursue this here, however.) With the use of (A1.12), the Kolmogorov entropy (A1.10) becomes the ideal entropy

$$S = -k_{\mathrm{B}} \sum_{j\alpha} \{f_{j\alpha}(1) \ln[f_{j\alpha}(1)] + f_{j\alpha}(0) \ln[f_{j\alpha}(0)]\} \tag{A1.13}$$

where, for normalization, we require $f_{j\alpha}(0) = 1 - f_{j\alpha}(1)$. The internal energy is the expectation of (A1.1) and this involves averages such as $\langle n_{j\alpha} \rangle$, $\langle n_{j\alpha} n_{j'\alpha'} \rangle$, $\langle n_{j\alpha} n_{j'\alpha'} n_{j''\alpha''} \rangle$,

etc. With the product form (A1.12) for joint probabilities these become simple products $f_{j\alpha}(1)$, $f_{j\alpha}(1)f_{j'\alpha'}(1)$, $f_{j\alpha}(1)f_{j'\alpha'}(1)f_{j''\alpha''}(1)$, etc, giving an internal energy

$$U = \sum_{j\alpha} f_{j\alpha}(1)E^{(1)}(j\alpha) + \frac{1}{2!}\sum_{j\alpha j'\alpha'} f_{j\alpha}(1)f_{j'\alpha'}(1)E^{(2)}(j\alpha, j'\alpha')$$

$$+ \frac{1}{3!}\sum_{j\alpha j'\alpha' j''\alpha''} f_{j\alpha}(1)f_{j'\alpha'}(1)f_{j''\alpha''}(1)E^{(3)}(j\alpha, j'\alpha', j''\alpha'')\ldots \quad (A1.14)$$

Using (A1.13), (A1.14) and (A1.4) we now have the trial quantity (A1.8) as a function of $\{f_{j\alpha}(1)\}$. The best mean-field state is obtained by minimizing separately with respect to each occupation probability $f_{j\alpha}(1)$:

$$0 = \frac{\partial\Omega}{\partial f_{k\gamma}(1)} = E^{(1)}(k\gamma) + \frac{2}{2!}\sum_{j'\alpha'} f_{j'\alpha'}(1)E^{(2)}(k\gamma, j'\alpha')$$

$$+ \frac{3}{3!}\sum_{j'\alpha' j''\alpha''} f_{j'\alpha'}(1)f_{j''\alpha''}(1)E^{(3)}(k\gamma, j'\alpha', j''\alpha'')\ldots$$

$$+ k_{\mathrm{B}}T\{\ln[f_{k\gamma}(1)] - \ln[1 - f_{k\gamma}(1)]\} - \mu - 3k_{\mathrm{B}}T\ln[Z_{\mathrm{vib}}(\beta, \omega_{k\gamma})]. \quad (A1.15)$$

In (A1.15), the extra factor of 3 in the triplet term comes from the three possibilities for matching $\{k, \gamma\}$ with one of the summation labels $j\alpha$, $j'\alpha'$, $j'''\alpha'''$ in (A1.1), and the symmetry of $E^{(3)}$ under permutation of its arguments has been assumed: similar arguments apply to the factor of 2 in the pair term. Rearranging (A1.15) we find that $f_{k\gamma}$ is a Gibbs distribution for a single site with an effective one-particle energy $\bar{\varepsilon}_{k\nu}$ and the actual chemical potential μ:

$$f_{k\gamma}(1) = \frac{\exp[-(\bar{\varepsilon} - \mu)/k_{\mathrm{B}}T]}{Q_{k\gamma}}[Z_{\mathrm{vib}}(\beta, \omega_{k\gamma})]^3 \quad (A1.16)$$

where

$$Q_{k\gamma} = 1 + \exp[-(\bar{\varepsilon}_{k\gamma} - \mu)/k_{\mathrm{B}}T][Z_{\mathrm{vib}}(\beta, \omega_{k\gamma})]^3 \quad (A1.17)$$

is the effective grand partition function for the site labelled k, γ, and

$$\bar{\varepsilon}_{k\gamma} = E^{(1)}(k\gamma) + \sum_{j'\alpha'} f_{j'\alpha'}(1)E^{(2)}(k\gamma, j'\alpha')$$

$$+ \frac{1}{2}\sum_{j'\alpha' j''\alpha''} f_{j'\alpha'}(1)f_{j''\alpha''}(1)E^{(3)}(k\gamma, j'\alpha', j''\alpha'') + \cdots \quad (A1.18)$$

is the effective one-site energy.

Equations (A1.11)–(A1.16) are valid even in inhomogeneous situations where $f_{j\alpha}$ depends on α, i.e. where f varies across the lattice. The above formalism could be used, for example, in a mean-field description of surface effects in H absorption. Here, however, we only consider the bulk properties and hence take $f_{j\alpha}(1) = \theta_j$ independent of location α within the crystal for each type j of absorption site. Then the mean-field distribution (A1.16) becomes

$$\theta_j = \frac{Z_j^3 \exp[-(\bar{\varepsilon}_j - \mu)/k_{\mathrm{B}}T]}{1 + Z_j^3 \exp[-(\bar{\varepsilon}_j - \mu)/k_{\mathrm{B}}T]} \quad (A1.19)$$

with

$$\bar{\varepsilon}_k = E^{(1)}(k) + \sum_{j'} \theta_{j'} \bar{V}_{2kj'} + \frac{1}{2} \sum_{j'j''} \theta_{j'}\theta_{j''} \bar{V}_{3kj'j''} + \cdots \tag{A1.20}$$

where

$$\bar{V}_{2kj} = \sum_{\alpha} E^{(2)}(k0, j\alpha) \tag{A1.21}$$

and

$$\bar{V}_{3kjl} = \sum_{\alpha\gamma} E^{(3)}(k0, j\alpha, l\gamma). \tag{A1.22}$$

In (A1.19), Z_j is the Einstein vibrational partition function (A1.7) for hydrogen on a site of type j; it is now assumed to be independent of location α within the lattice.

The interpretation of (A1.16) or (A1.19) involves an independent site at which an absorbed hydrogen feels an effective one-body potential $\bar{\varepsilon}$; $\bar{\varepsilon}$ depends on the average occupations of other sites.

One can of course postulate (A1.16) or (A1.19) directly, but the above variational treatment has a number of advantages. Firstly, the coefficients $\bar{V}_2$, $\bar{V}_3$, ... are related in an unambiguous way to the microscopic energies $E(\{n_{j\alpha}\})$ (see (A1.1), (A1.21) and (A1.22)). Secondly, the variational approach gives expressions for the entropy, internal energy and free energy by substituting the optimal $\{f_{j\alpha}\}$ into (A1.13) and (A1.14). In particular, for a homogeneous situation,

$$U = \sum_j N_j\theta_j \left(E^{(1)}(j) + \frac{1}{2!} \sum_{j'} \theta_{j'} \bar{V}_{2jj'} + \frac{1}{3!} \sum_{j'j''} \theta_{j'}\theta_{j''} \bar{V}_{3jj'j''} + \cdots \right) \tag{A1.23}$$

and

$$S = \sum_j N_j[\theta_j \ln(\theta_j) - (1 - \theta_j)\ln(1 - \theta_j)]. \tag{A1.24}$$

Thirdly, the above quantities when substituted into (A1.8) give a rigorous bound on the potential Ω, because of the variational nature of this theory.

Appendix 2. Considerations for decomposition of the energy into additive site, pair, triplet, ..., contributions

Consider a metal lattice with N hydrogen absorption sites divided into inequivalent classes $j = 1, 2, 3 \ldots$ (e.g. $j = 1$ and $j = 2$ might represent octahedral and tetrahedral sites, respectively). We define the configurational state of the lattice–hydrogen system by the occupation numbers $n_{j\alpha} = 0$ or 1 where, for each j value, α runs from 1 to N_j, N_j being the number of absorption sites of type j. Then there exists an energy function $E(\{n_{j\alpha}\})$ which is the energy of a microscopic configuration of H on the lattice, including all electronic energies plus any energy of (static) lattice deformation caused by the presence of the hydrogen atoms. We now proceed to define single-site, pair, triplet, ..., energies $E^{(1)}$, $E^{(2)}$, $E^{(3)}$, ..., in a specific manner.

(1) Consider first the case where all $n_{j\alpha} = 0$. The energy in this case will be denoted $E^{(0)}(N)$; it is the energy (except vibrational energy) of the pure metal lattice, i.e. it is $E(\{\text{all } n_{j\alpha} = 0\})$.

(2) Consider next the case where all $n_{j\alpha} = 0$ except for $n_{J\gamma} = 1$. The single-site energy $E^{(1)}$ is defined as

$$E^{(1)}(J\gamma) = E(\text{all } n_{j\alpha} = 0 \text{ except } n_{J\gamma} = 1) - E^{(0)}(N). \qquad \text{(A2.1)}$$

In principle, $E^{(1)}(J\gamma)$ depends on the location within the crystal γ and the size and shape of the whole metal sample (because of surface effects, for example). However, for bulk properties, we shall assume that the sample is dominated by 'interior' absorption sites sufficiently far from the surface that properly extensive behaviour is seen. Under these circumstances, $E^{(1)}(J, \gamma)$ is expected to depend on the type J of the site in question but not significantly on the location γ of the site in the crystal.

(3) Consider next the case where all $n_{j\alpha} = 0$ except for two occupied sites corresponding to $\alpha = \gamma$ and $\alpha = \delta$, so that $n_{J\gamma} = 1$ and $n_{K\delta} = 1$. Then we define a pair interaction energy $E^{(2)}$ by

$$E^{(2)}(J\gamma, K\delta) = E(\{\text{all } n_{j\alpha} = 0 \text{ except } n_{J\gamma} = 1, n_{K\delta} = 1\}) - E^{(0)} - E^{(1)}(J\gamma) - E^{(1)}(K\delta).$$
$$\text{(A2.2)}$$

Again we assume that there is a majority of 'bulk' sites far from a surface where $E^{(2)}$ behaves extensively, i.e. depends only on separation (distance and possibly direction) between the sites $J\gamma$ and $K\delta$. This assumption neglects a small effect, namely the change in the average electron density on addition of a second H atom, which will slightly change the most appropriate value of $E^{(1)}$ to be subtracted in (A2.2), because the ultimate origin of H energetics in the metal is electronic: see also appendix 1.

(4) Consider next the case where all $n_{j\alpha} = 0$ except for three occupied sites, so that $n_{J\gamma} = 1$, $n_{K\delta} = 1$ and $n_{L\varepsilon} = 1$. Then we define a triplet interaction energy $E^{(3)}$ by

$$E^{(3)}(J\gamma, K\delta, L\varepsilon) = E(\{\text{all } n_{j\alpha} = 0 \text{ except } n_{J\gamma} = 1, n_{K\delta} = 1, n_{L\varepsilon} = 1\})$$
$$- E^{(0)} - E^{(1)}(J\gamma) - E^{(1)}(K\delta) - E^{(1)}(L\varepsilon)$$
$$- E^{(2)}(J\gamma, K\delta) - E^{(2)}(J\gamma, L\varepsilon) - E^{(2)}(K\delta, L\varepsilon). \qquad \text{(A2.3)}$$

Again we assume that there is a majority of 'bulk' sites far from a surface where $E^{(3)}$ is a function only of relative locations, and we neglect the change in average electron density on the values of $E^{(1)}$ and $E^{(2)}$ to be subtracted in (A2.3).

(5) The set of equations (A2.1), (A2.2) and (A2.3) can obviously be extended to define interactions $E^{(n)}$ among n electrons at a time. The same type of equation, and assumption of extensiveness should be appropriate as long as the fractional H occupation is sufficiently low that the change in average electron density does not significantly alter the appropriate values of the $E^{(i)}$. We shall assume that we are in such a low-occupation regime. Out of this regime it may be possible to maintain the same type of description provided that one refers energies to a state in which the average electron density is held constant by a Maxwell demon suitably compressing or expanding the crystal lattice.

Finally, the type of equation that we have introduced to define the $\{E^N\}$, plus the assumption of extensiveness, guarantees an expansion of the total E in terms of singlet, pairs, triplet, ..., energies; to see this, one merely needs to transpose the series of equations (A2.1), (A2.2), (A2.3), ..., so that E stands alone on one side of the equation. It would be interesting to find out from microstructure theory how good is the assumption of extensiveness as used here.

References

[1] Guggenheim E A 1935 *Proc. R. Soc.* A **144** 304
[2] Bethe E 1935 *Proc. R. Soc.* A **150** 552
[3] Dietrich S and Wagner H 1979 *Z. Phys.* B **36** 121
[4] Alefeld G 1972 *Ber. Bunsenges. Phys. Chem.* **76** 746
[5] Christensen O B, Stoltze P, Jacobsen K W and Nørskov J K 1990 *Phys. Rev.* B **41** 12413
[6] Switendick A C 1978 *Sandia Laboratories, Albuquerque, NM, Report* SAND 78-0250
[7] Salomons E 1990 *J. Phys.: Condens. Matter* **2** 845
[8] Lacher J R 1937 *Proc. R. Soc.* A **161** 525
[9] Feenstra R, Griessen R and de Groot D G 1986 *J. Phys. F: Met. Phys.* **16** 1933
[10] Blaurock J 1985 *Dissertation* Münster
[11] Wicke E and Blaurock J 1987 *J. Less-Common Met.* **130** 355
[12] Oates W A and Stoneham A M 1983 *J. Phys. F: Met. Phys.* **13** 2427
[13] Lee K Y 1993 *PhD Thesis* University of Newcastle, Australia
[14] Salomons E, Hemmes H and Griessen R 1990 *J. Phys.: Condens. Matter* **2** 817
[15] Oates W A 1993 Private communication
[16] Kisi E H, Buckley C E and Gray E M 1992 *J. Alloys Compounds* **185** 369
[17] Flanagan T B and Oates W A 1991 *Ann. Rev. Mater. Sci.* **21** 269
[18] Tewary V K 1973 *Adv. Phys.* **22** 757